Magneto-Structural Correlation Studies and Theoretical Calculations of a Unique Family of Single End-to-End Azide-Bridged Ni-4(II) Cyclic Clusters

7 AUTHORS, INCLUDING:

Sujit Sasmal
Indian Institute of Technology Kanpur
18 PUBLICATIONS **317** CITATIONS

SEE PROFILE

Susanta Hazra
Technical University of Lisbon
38 PUBLICATIONS **514** CITATIONS

SEE PROFILE

Eliseo Ruiz
University of Barcelona
205 PUBLICATIONS **8,137** CITATIONS

SEE PROFILE

Inorganic Chemistry

Article

Magneto-Structural Correlation Studies and Theoretical Calculations of a Unique Family of Single End-to-End Azide-Bridged Ni$_4^{II}$ Cyclic Clusters

Sujit Sasmal,[†] Susanta Hazra,[†] Parimal Kundu,[‡] Samit Majumder,[†] Núria Aliaga-Alcalde,*[,§] Eliseo Ruiz,*[,‖] and Sasankasekhar Mohanta*[,†]

[†]*Department of Chemistry, University of Calcutta, 92 A. P. C Road, Kolkata 700 009, India,* [‡]*Department of Chemistry, Maharaja Manindra Chandra College, 20 Ramkanto Bose Street, Kolkata 700 003, India,* [§]*ICREA-Departament de Química Inorgànica, Universitat de Barcelona, Diagonal 647, 08028 Barcelona, Spain, and* [‖]*Departament de Química Inorgànica and Institut de Química Teòrica i Computacional, Universitat de Barcelona, Diagonal 647, 08028 Barcelona, Spain*

The work in this paper aims to portray a complete structural, magnetic, and theoretical description of two original end-to-end (EE) $\mu_{1,3}$-azide-bridged, cyclic tetranuclear Ni^{II} clusters, [{Ni^{II}(L^1)($\mu_{1,3}$-N$_3$)(H$_2$O)}$_4$] (**1**) and [{Ni^{II}(L^2)($\mu_{1,3}$-N$_3$)(H$_2$O)}$_4$] (**2**), where the ligands used to achieve these species, HL^1 and HL^2, are the tridentate Schiff base ligands obtained from [1 + 1] condensations of salicylaldehyde with 1-(2-aminoethyl)-piperidine and 4-(2-aminoethyl)-morpholine, respectively. The title compounds, **1** and **2**, crystallize in a monoclinic *P*2$_1$ space group. Overall, both species can be described in a similar way; where all Ni^{II} centers within each molecule are hexacoordinated and bound to [L^1]$^-$ or [L^2]$^-$ through the phenoxo oxygen, imine nitrogen, and piperidine/morpholine nitrogen atoms of the corresponding ligand. The remaining coordination sites are satisfied by one molecule of H$_2$O and two nitrogen atoms from N$_3^-$ anions. The latest act as bridges between Ni^{II} ions, and eventually, only four azido groups are linked to the same number of Ni^{II} centers resulting in the formation of cyclic Ni$^{II}_4$ systems. Interestingly, compounds **1** and **2** are the two sole examples of tetranuclear clusters generated exclusively by EE azide-bridging ligands to date. All the N(azide)−Ni−N(azide) moieties are almost linear in **1** and **2** indicating trans arrangement of the azido ligand. Variable-temperature (2−300 K) magnetic susceptibilities of **1** and **2** have been measured under magnetic fields of 0.04 T (from 2 to 30 K) and 0.7 T (from 30 to 300 K), and magneto-structural correlations have been performed. Despite the presence of both ferromagnetic and antiferromagnetic interactions in both compounds, significant differences have been observed in their magnetic behaviors directly related to the arrangement of the bridging azido ligands. Hence, compound **1** has an overall moderate antiferromagnetic behavior due to the presence of an exchange pathway with an unprecedented Ni−N···N−Ni torsion angle close to 0°, meanwhile complex **2** exhibits a predominant ferromagnetic behavior, with torsion angles between 50 and 90°. Density functional theory calculations have been performed to provide more insight into the magnetic nature of this new family of Ni^{II}−azido complexes and also to corroborate the fitting of the data.

Introduction

Supramolecular chemistry and crystal engineering of co-ordination compounds are of current interest due to the fascinating structural diversity and the potential applications as functional materials.[1] In general, the different molecular architectures depend mainly on three factors: the structural functionality of their ligands, the coordination geometry of the metal centers, and the weak intermolecular lattice interactions.[2−6] Taking advantage of these factors, the development

of organic−inorganic hybrid materials aims to combine the physical and chemical properties of inorganic and organic

*Corresponding authors. E-mail: sm_cu_chem@yahoo.co.in (S.M.), nuria.aliaga@icrea.cat (N.A.-A.).

(1) (a) Lehn, J.-M. *Supramolecular Chemistry*, VCH: Weinheim, Germany, 1995. (b) Yaghi, O. M.; Li, G.; Li, H. *Nature* **1995**, *378*, 703–706. (c) Neumann, R.; Dahan, M. *Nature* **1997**, *388*, 353–355. (d) Beer, P. D.; Gale, P. A. *Angew. Chem., Int. Ed.* **2001**, *40*, 486–516. (e) Shimomura, S.; Higuchi, M.; Matsuda, R.; Yoneda, K.; Hijikata, Y.; Kubota, Y.; Mita, Y.; Kim, J.; Takata, M.; Kitagawa, S. *Nat. Chem.* **2010**, *2*, 633–637.

(2) (a) Robson, R. *J. Chem. Soc., Dalton Trans.* **2000**, 3735–3744. (b) Decurtins, S.; Pellaux, R.; Antorrena, G.; Palacio, F. *Coord. Chem. Rev.* **1999**, *841*, 190–192. (c) Song, Y.; Massera, C.; Roubeau, O.; Gamez, P.; Manotti-Lanfredi, A. M.; Reedijk, J. *Inorg. Chem.* **2004**, *43*, 6842–6847.

(3) (a) *Transition Metals in Supramolecular Chemistry*; Perspectives in Supramolecular Chemistry 5; Sauvage, J.-P., Ed.; Wiley: London, 1999. (b) Blake, A. J.; Champness, N. R.; Hubberstey, P.; Withersby, M. A.; Schröder, M. *Coord. Chem. Rev.* **1999**, *183*, 117–138. (c) Lin, H.-H.; Mohanta, S.; Lee, C.-J.; Wei, H.-H. *Inorg. Chem.* **2003**, *42*, 1584–1589.

(4) Ribas, J.; Escuer, A.; Monfort, M.; Vicente, R.; Cortés, R.; Lezama, L.; Rojo, T. *Coord. Chem. Rev.* **1999**, *193−195*, 1027–1068.

(5) (a) Verdaguer, M.; Bleuzen, A.; Marvaud, V.; Vaissermann, J.; Seuleiman, M.; Desplanches, C.; Scuiller, A.; Train, C.; Garde, R.; Galley, G.; Lomenech, C.; Rosenman, I.; Veillet, P.; Cartier, C.; Villain, F. *Coord. Chem. Rev.* **1999**, *190−192*, 1023–1047. (b) Ohba, M.; Ōkawa, H. *Coord. Chem. Rev.* **2000**, *198*, 313–328. (c) Batten, S. R.; Murray, K. S. *Coord. Chem. Rev.* **2003**, *246*, 103–130.

components.[1,4] The above-mentioned features are also increasingly applied in other current areas of investigation, for instance in the interdisciplinary area of molecular magnetism,[4,5,7−32] where major efforts are applied in the study of magneto-structural correlations of metallospecies with the aim of understanding and controlling the final systems and their properties. Relating to both the fields of molecular magnetism and supramolecular chemistry/crystal engineering, a great deal of effort has recently been devoted to develop or utilize novel polydentate blocking and bridging ligands that can accommodate metal ions and to create unique supramolecular structures and new network topologies at all sorts of levels [from zero- to three-dimensional (0D and 3D, respectively)]. To develop varieties of topologies, Schiff bases[5b,6,7,33] and azide anions[4,7,10−31,33] are known to behave excellently as blocking and bridging ligands, respectively.

Metallo-azido species have been always of great interest in the above-mentioned two fields of research due to a number of coordination modes of this potentially bridging ligand as well as due to its ability to mediate ferro- or antiferromagnetic interactions among metal centers. The most usual bridging modes are the end-on ($\mu_{1,1}$-, commonly expressed as EO)[4,7,10−18] and end-to-end ($\mu_{1,3}$-, EE),[4,7,12,19−26] but some others like, $\mu_{1,1,1}$-,[13,16,27,28] $\mu_{1,1,3}$-,[14,19,28,29] $\mu_{1,1,1,1}$-,[30] and $\mu_{1,1,3,3}$-[31] have been also described in the past. This way, a number of azide-bridged systems of different nuclearity (di-, oligo-, and polynuclear clusters) and also of 1D, 2D, and 3D topologies have been achieved.[4,7,10−31,33] As a result, there is a considerable amount of information available on experimental[4,10,24e] and theoretical[32] magneto-structural correlations of azido species, which often exhibit appealing features, for example, long-range magnetic ordering.[4,11c,17,18b,d,f,20]

Despite all the encouraging results, the serendipitous nature of most of the compounds containing azido-bridging ligands brings out the moderate freedom in the design of the final structures.[4,7,10−31,33] As remarked before, several features may rule the assemblage to afford the products, and

(6) (a) Nayak, M.; Koner, R.; Lin, H.-H.; Flörke, U.; Wei, H.-H.; Mohanta, S. *Inorg. Chem.* **2006**, *45*, 10764. (b) Hazra, S.; Koner, R.; Nayak, M.; Sparkes, H. A.; Howard, J. A. K.; Mohanta, S. *Cryst. Growth Des.* **2009**, *9*, 3603–3608. (c) Nayak, M.; Jana, A.; Fleck, M.; Hazra, S.; Mohanta, S. *CrystEngComm* **2010**, *12*, 1416–1421.

(7) Kahn, O. *Molecular Magnetism*; VCH Publications: New York, 1993.

(8) (a) *Single-Molecule Magnets and Related Phenomena*; Winpenny, R., Ed.; Springer: Berlin, Heidelberg, Germany, 2006. (b) *Magnetism: Molecules to Materials II*, Miller, J. S., Drillon, M., Eds.; Willey-VCH: Weinheim, Germany, 2001.

(9) (a) Bechlars, B.; D'Alessandro, D. M.; Jenkins, D. M.; Iavarone, A. T.; Glover, S. D.; Kubiak, C. P.; Long, J. R. *Nat. Chem.* **2010**, *2*, 362–368. (b) Ribas-Arino, J.; Baruah, T.; Pederson, M. R. *J. Am. Chem. Soc.* **2006**, *128*, 9497–9505.

(10) Koner, R.; Hazra, S.; Fleck, M.; Jana, A.; Lucas, C. R.; Mohanta, S. *Eur. J. Inorg. Chem.* **2009**, 4982–4988.

(11) (a) Yang, C.-I.; Wernsdorfer, W.; Lee, G.-H.; Tsai, H.-L. *J. Am. Chem. Soc.* **2007**, *129*, 456–457. (b) Milios, C. J.; Inglis, R.; Vinslava, A.; Prescimone, A.; Parsons, S.; Perlepes, S. P.; Christou, G.; Brechin, E. K. *Chem. Commun.* **2007**, 2738–2740. (c) Feng, P. L.; Stephenson, C. J.; Amjad, A.; Ogawa, G.; Barco, E. d.; Hendrickson, D. N. *Inorg. Chem.* **2010**, *49*, 1304–1306.

(12) Demeshko, S.; Leibeling, G.; Dechert, S.; Meyer, F. *Dalton Trans.* **2006**, 3458–3465.

(13) Milios, C. J.; Prescimone, A.; Sanchez-Benitez, J.; Parsons, S.; Murrie, M.; Brechin, E. K. *Inorg. Chem.* **2006**, *45*, 7053–7055.

(14) Demeshko, S.; Leibeling, G.; Maringgele, W.; Meyer, F.; Mennerich, C.; Klauss, H.-H.; Pritzkow, H. *Inorg. Chem.* **2005**, *44*, 519–528.

(15) (a) Liu, G.-F.; Ren, Z.-G.; Li, H.-X.; Chen, Y.; Li, Q.-H.; Zhang, Y.; Lang, J.-P. *Eur. J. Inorg. Chem.* **2007**, 5511–5522. (b) Mandal, D.; Mikuriya, M.; Fun, H.-K.; Ray, D. *Inorg. Chem. Commun.* **2007**, *10*, 657–660. (c) Escuer, A.; Goher, M. A. S.; Mautner, F. A.; Vicente, R. *Inorg. Chem.* **2000**, *39*, 2107–2112. (d) Ma, D.-q.; Hikichi, S.; Akita, M.; Moro-oka, Y. *J. Chem. Soc., Dalton Trans.* **2000**, 1123–1134.

(16) (a) Zhang, Y.-Z.; Wernsdorfer, W.; Pan, F.; Wang, Z.-M.; Gao, S. *Chem. Commun.* **2006**, 3302–3304. (b) Karmakar, T. K.; Chandra, S. K.; Ribas, J.; Mostafa, G.; Lu, T. H.; Ghosh, B. K. *Chem. Commun.* **2002**, 2364–2365.

(17) Gu, Z.-G.; Song, Y.; Zuo, J.-L.; You, X.-Z. *Inorg. Chem.* **2007**, *46*, 9522–9524.

(18) (a) Liu, F.-C.; Zeng, Y.-F.; Zhao, J.-P.; Hu, B.-W.; Bu, X.-H.; Ribas, J.; Cano, J. *Inorg. Chem.* **2007**, *46*, 1520–1522. (b) Wang, X.-Y.; Wang, L.; Wang, Z.-M.; Gao, S. *J. Am. Chem. Soc.* **2006**, *128*, 674–675. (c) Bitschnau, B.; Egger, A.; Escuer, A.; Mautner, F. A.; Sodin, B.; Vicente, R. *Inorg. Chem.* **2006**, *45*, 868–876. (d) Gao, E.-Q.; Yue, Y.-F.; Bai, S.-Q.; He, Z.; Yan, C.-H. *J. Am. Chem. Soc.* **2004**, *126*, 1419–1429. (e) Leibeling, G.; Demeshko, S.; Bauer-Siebenlist, B.; Meyer, F.; Pritzkow, H. *Eur. J. Inorg. Chem.* **2004**, 2413–2420. (f) Yoon, J. H.; Ryu, D. W.; Kim, H. C.; Yoon, S. W.; Suh, B. J.; Hong, C. S. *Chem.—Eur. J.* **2009**, *15*, 3661–3665.

(19) Meyer, F.; Demeshko, S.; Leibeling, G.; Kersting, B.; Kaifer, E.; Pritzkow, H. *Chem.—Eur. J.* **2005**, *11*, 1518–1526.

(20) Gao, E.-Q.; Liu, P.-P.; Wang, Y.-Q.; Yue, Q.; Wang, Q.-L. *Chem.—Eur. J.* **2009**, *15*, 1217–1226.

(21) (a) Hong, C. S.; Koo, J.-e.; Son, S.-K.; Lee, Y. S.; Kim, Y.-S.; Do, Y. *Chem.—Eur. J.* **2001**, *7*, 4243–4252. (b) Escuer, A.; Castro, I.; Mautner, F.; Fallah, M. S. E.; Vicente, R. *Inorg. Chem.* **1997**, *36*, 4633–4640. (c) Monfort, M.; Resino, I.; Fallah, M. S. E.; Ribas, J.; Solans, X.; Font-Bardía, M.; Stoeckli-Evans, H. *Chem.—Eur. J.* **2001**, *7*, 280–287. (d) Hong, C. S.; Do, Y. *Angew. Chem., Int. Ed.* **1999**, *38*, 193–195.

(22) (a) McLachlan, G. A.; Fallon, G. D.; Martin, R. L.; Moubaraki, B.; Murray, K. S.; Spiccia, L. *Inorg. Chem.* **1994**, *33*, 4663–4668. (b) Zhang, Z.-H.; Bu, X.-H.; Ma, Z.-H.; Bu, W.-M.; Tang, Y.; Zhao, Q.-H. *Polyhedron* **2000**, *19*, 1559–1566.

(23) (a) Kersting, B.; Steinfeld, G.; Siebert, D. *Chem.—Eur. J.* **2001**, *7*, 4253–4258. (b) Leibeling, G.; Demeshko, S.; Dechert, S.; Meyer, F. *Angew. Chem., Int. Ed.* **2005**, *44*, 7111–7114.

(24) (a) Mukherjee, P. S.; Dalai, S.; Zangrando, E.; Lloret, F.; Chaudhuri, N. R. *Chem. Commun.* **2001**, 1444–1445. (b) Goher, M. A. S.; Escuer, A.; Mautner, F. A.; Al-Salem, N. A. *Polyhedron* **2002**, *21*, 1871–1876. (c) Escuer, A.; Vicente, R.; Ribas, J.; Fallah, M. S. E.; Solans, X. *Inorg. Chem.* **1993**, *32*, 1033–1035. (d) Fallah, M. S. E.; Escuer, A.; Vicente, R.; Solans, X.; Font-Bardía, M.; Verdaguer, M. *Inorg. Chim. Acta* **2003**, *344*, 133–142. (e) Liu, X.-T.; Wang, X.-Y.; Znang, W.-X.; Cui, P.; Gao, S. *Adv. Mater.* **2006**, *18*, 2852–2856.

(25) (a) Escuer, A.; Vicente, R.; Ribas, J.; Fallah, M. S. E.; Solans, X.; Font-Bardía, M. *Inorg. Chem.* **1994**, *33*, 1842–1847. (b) Monfort, M.; Ribas, J.; Solans, X.; Font-Bardía, M. *Inorg. Chem.* **1996**, *35*, 7633–7638. (c) Escuer, A.; Vicente, R.; Fallah, M. S. E.; Ribas, J.; Solans, X.; Font-Bardía, M. *J. Chem. Soc., Dalton Trans.* **1993**, 2975–2976. (d) Monfort, M.; Resino, I.; Ribas, J.; Solans, X.; Font-Bardía, M.; Stoeckli-Evans, H. *New J. Chem.* **2002**, *26*, 1601–1606. (e) Vicente, R.; Escuer, A.; Ribas, J.; Fallah, M. S. E.; Solans, X.; Font-Bardía, M. *Inorg. Chem.* **1995**, *34*, 1278–1281. (f) Ribas, J.; Monfort, M.; Diaz, C.; Bastos, C.; Mer, C.; Solans, X. *Inorg. Chem.* **1995**, *34*, 4986–4990.

(26) (a) Massoud, S. S.; Mautner, F. A.; Vicente, R.; Gallo, A. A.; Ducasse, E. *Eur. J. Inorg. Chem.* **2007**, 1091–1102. (b) Cortes, R.; Urtiaga, K.; Lezama, L.; Pizarro, J. L.; Goni, A.; Arriortua, M. I.; Rojo, T. *Inorg. Chem.* **1994**, *33*, 4009–4015. (c) Ribas, J.; Monfort, M.; Ghosh, B. K.; Cortes, R.; Solans, X.; Font-Bardía, M. *Inorg. Chem.* **1996**, *35*, 864–868.

(27) (a) Stamatatos, T. C.; Abboud, K. A.; Wernsdorfer, W.; Christou, G. *Angew. Chem., Int. Ed.* **2006**, *45*, 4134–4137. (b) Aromí, G.; Parsons, S.; Wernsdorfer, W.; Brechin, E. K.; McInnes, E. J. L. *Chem. Commun.* **2005**, 5038–5040.

(28) Bell, A.; Aromí, G.; Teat, S. J.; Wernsdorfer, W.; Winpenny, R. E. P. *Chem. Commun.* **2005**, 2808–2810.

(29) Demeshk, S.; Leibeling, G.; Dechert, S.; Fuchs, S.; Pruschke, T.; Meyer, F. *Chem. Phys. Chem.* **2007**, *8*, 405–417.

(30) (a) Papaefstathiou, G. S.; Perlepes, S. P.; Escuer, A.; Vicente, R.; Font-Bardía, M.; Solans, X. *Angew. Chem., Int. Ed.* **2001**, *40*, 884–886. (b) Papaefstathiou, G. S.; Escuer, A.; Vicente, R.; Font-Bardía, M.; Solans, X.; Perlepes, S. P. *Chem. Commun.* **2001**, 2414–2415.

(31) Meyer, F.; Kircher, P.; Pritzkow, H. *Chem. Commun.* **2003**, 774–775.

(32) (a) Ruiz, E.; Cano, J.; Alvarez, S.; Alemany, P. *J. Am. Chem. Soc.* **1998**, *120*, 11122–11129. (b) Manca, G.; Cano, J.; Ruiz, E. *Inorg. Chem.* **2009**, *48*, 3139–3144. (c) Fabrizi de Biani, F.; Ruiz, E.; Cano, J.; Novoa, J. J.; Alvarez, S. *Inorg. Chem.* **2000**, *39*, 3221–3229. (d) Triki, S.; Gómez-García, C. J.; Ruiz, E.; Sala-Pala, J. *Inorg. Chem.* **2005**, *44*, 5501–5508.

(33) (a) Gao, E.-Q.; Bai, S.-Q.; Wang, Z.-M.; Yan, C.-H. *J. Am. Chem. Soc.* **2003**, 4984–4985. (b) Li, W.; Li, Z.; Li, L.; Liao, D.; Jiang, Z. *J. Solid State Chem.* **2007**, *180*, 2973–2977. (c) Stamatatos, T. C.; Abboud, K. A.; Perlepes, S. P.; Christou, G. *Dalton Trans.* **2007**, 3861–3863. (d) Darensbourg, D. J.; Frantz, E. B. *Inorg. Chem.* **2007**, *46*, 5967–5978.

therefore new topologies may be attained by modifying these parameters. Among them, this work focuses on the impact of N_3^- ions in combination with chelating coligands HL^1 and HL^2 (Scheme 1) in the chemistry of nickel(II), where the ligands are the [1 + 1] condensation products of salicylaldehyde and 1-(2-aminoethyl)-piperidine (for HL^1) or 4-(2-aminoethyl)-morpholine (for HL^2). Although the phenoxo groups of $[L^1]^-$ and $[L^2]^-$ may function as bridging ligands, both $[L^1]^-$ and $[L^2]^-$ should behave as tridentate blocking units, where the nitrogen atoms from the piperidine or morpholine together with the oxygen atom from the phenoxo coordinate to the same metal center, here, nickel(II). It has been already mentioned that predictions are complicated in the metallo-azido chemistry, and therefore, as nickel(II)−azide chemistry with the two ligands HL^1 and HL^2 has not been investigated so far, interesting topology and properties may be achieved in the nickel(II)−azide compounds derived from these two ligands. With these expectations, HL^1 and HL^2 were reacted with $Ni(ClO_4)_2 \cdot 6H_2O$ and NaN_3, respectively, and consequently, two novel tetranuclear nickel(II) clusters, $[\{Ni^{II}(L^1)(\mu_{1,3}\text{-}N_3)(H_2O)\}_4]$ (**1**) and $[\{Ni^{II}(L^2)(\mu_{1,3}\text{-}N_3)(H_2O)\}_4]$ (**2**), displaying unprecedented topological aspects were obtained. Herein, we report the synthetic procedure and X-ray crystallography of **1** and **2** as well as the study of the magnetic properties and density functional theory (DFT) calculations of these two new complexes.

Experimental Section

Materials and Physical Measurements. All the reagents and solvents were purchased from the commercial sources and used as received. Elemental (C, H, and N) analyses were performed on a Perkin-Elmer 2400 II analyzer. IR spectra were recorded in the region of 400−4000 cm^{-1} on a Bruker-Optics Alpha-T spectrophotometer with samples as KBr disks. Magnetic susceptibility measurements were carried out on polycrystalline samples with a DSM5 Quantum Design magnetometer working in the range 2−300 K under magnetic fields of 0.04 and 0.7 T (from 2 to 30 and 30 to 300 K, respectively). Diamagnetic corrections were estimated from Pascal Tables. TIP is the temperature-independent paramagnetism. R is the agreement factor defined as $R = \Sigma_i[(\chi_M T)_{obs(i)} - (\chi_M T)_{calc(i)}]^2 / \Sigma_i[(\chi_M T)_{obs(i)}]^2$.

Computational Details. Electronic structure calculations based on DFT provide an excellent estimation of the exchange coupling constants in polynuclear transition-metal complexes, taking into account the tiny involved energy differences.[34] Since a detailed description of the computational strategy used to calculate the exchange coupling constants in polynuclear complexes is outside the scope of this paper, we will focus our discussion here to its most relevant aspects. Previously, we have published a series of papers devoted to such purpose where more details can be found.[35−37] For the studied Ni$_4$ complexes, **1** and **2**, there are four first-neighbor exchange interactions, we neglected the next-nearest neighbor interactions. We employed six spin configurations to estimate these four J values, the high spin solution (S = 4), two S = 2 wave functions obtained with the spin inversion of the Ni(1) and Ni(4), respectively, and finally

Scheme 1. Chemical Structure of HL^1 and HL^2
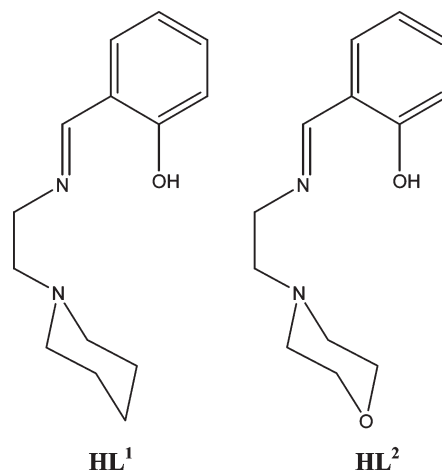
three S = 0 spin configurations for the inversion of the following pairs {Ni(1), Ni(3)}, {Ni(1), Ni(4)}, and {Ni(3), Ni(4)}.

In previous papers, we have analyzed the effect of the basis set and the choice of the functional on the accuracy of the determination of the exchange coupling constants.[36−38] Thus, we found that the hybrid B3LYP functional,[39] together with the basis sets proposed by Schaefer et al., provide J values in excellent agreement with the experimental ones. The hybrid character of the B3LYP due to the inclusion of some contribution of exact exchange reduces self-interaction error improving the calculated J values in comparison with non-hybrid functionals. We have employed a basis set of triple-ζ quality as proposed by Schaefer et al.[40] The calculations were performed with the Gaussian09 code,[41] using guess functions generated with the Jaguar 7.0 code[42] introducing the ligand field effects,[43] in order to control the local charge and multiplicity of each atom.

Synthesis of $[\{Ni^{II}(L^1)(\mu_{1,3}\text{-}N_3)(H_2O)\}_4]$ (1) and $[\{Ni^{II}(L^2)(\mu_{1,3}\text{-}N_3)(H_2O)\}_4]$ (2). These two compounds were prepared following the exact procedure described below for **1**, although in the synthesis of **2**, 4-(2-aminoethyl)-morpholine was used instead of 1-(2-aminoethyl)-piperidine.

A slurry of 1-(2-aminoethyl)-piperidine (0.128 g, 1 mmol) in MeOH (10 mL) was added to a solution of salicylaldehyde (0.122 g, 1 mmol) in MeOH (20 mL). The mixture was refluxed for 2 h, and the volume of the resulting red-colored solution was reduced to 10 mL. Then, a methanolic solution (5 mL) of $NiClO_4 \cdot 6H_2O$ (0.366 g, 1 mmol) was added dropwise, and the

(34) (a) Ruiz, E.; Alemany, P.; Alvarez, S.; Cano, J. *J. Am. Chem. Soc.* **1997**, *119*, 1297–1303. (b) Ruiz, E.; Cano, J.; Alvarez, S. *Chem.—Eur. J.* **2005**, *11*, 4767–4771. (c) Ruiz, E.; Cauchy, T.; Cano, J.; Costa, R.; Tercero, J.; Alvarez, S. *J. Am. Chem. Soc.* **2008**, *130*, 7420–7426.

(35) Ruiz, E. *Struct. Bonding (Berlin)* **2004**, *113*, 71–102. (b) Ruiz, E.; Alvarez, S.; Cano, J.; Polo, V. *J. Chem. Phys.* **2005**, *123*, 164110(1)–164110(7).

(36) Ruiz, E.; Cano, J.; Alvarez, S.; Alemany, P. *J. Comput. Chem.* **1999**, *20*, 1391–1400.

(37) Ruiz, E.; Rodríguez-Fortea, A.; Cano, J.; Alvarez, S.; Alemany, P. *J. Comput. Chem.* **2003**, *24*, 982–989.

(38) Ruiz, E.; Rodríguez-Fortea, A.; Tercero, J.; Cauchy, T.; Massobrio, C. *J. Chem. Phys.* **2005**, *123*, 074102(1)–074102(10).

(39) Becke, A. D. *J. Chem. Phys.* **1993**, *98*, 5648–5652.

(40) Schaefer, A.; Huber, C.; Ahlrichs, R. *J. Chem. Phys.* **1994**, *100*, 5829–5835.

(41) Frisch, M. J.; Trucks, G. W.; Schlegel, H. B.; Scuseria, G. E.; Robb, M. A.; Cheeseman, J. R.; Scalmani, G.; Barone, V.; Mennucci, B.; Petersson, G. A.; Nakatsuji, H.; Caricato, M.; Li, X.; Hratchian, H. P.; zmaylov, A. F.; Bloino, I. J.; Zheng, G.; Sonnenberg, J. L.; Hada, M.; Ehara, M.; Toyota, K.; Fukuda, R.; Hasegawa, J.; Ishida, M.; Nakajima, T.; Honda, Y.; Kitao, O.; Nakai, H.; Vreven, T.; Montgomery, J. J. A.; Peralta, J. E.; Ogliaro, F.; Bearpark. M.; Heyd, J. J.; Brothers, E.; Kudin, K. N.; Staroverov, V. N.; Kobayashi, R.; Normand, J.; Raghavachari, K.; Rendell, A.; Burant, J. C.; Iyengar, S. S.; Tomasi, J.; Cossi, M.; Rega, N.; Millam, J. M.; Klene, M.; Knox, J. E.; Cross, J. B.; Bakken, V.; Adamo, C.; Jaramillo, J.; Gomperts, R.; Stratmann, R. E.; Yazyev, O.; Austin, A. J.; Cammi, C.; Pomelli, J. W.; Ochterski, R.; Martin, R. L.; Morokuma, K.; Zakrzewski, V. G.; Voth, G. A.; Salvador, P.; Dannenberg, J. J.; Dapprich, S.; Daniels, A. D.; Farkas, O.; Foresman, J. B.; Ortiz, J. V.; Cioslowski, J.; Fox, D. J. *Gaussian 09*, revision A.1; Gaussian, Inc.: Wallingford, CT, 2009.

(42) *Jaguar 7.0*; Schrödinger, LLC: New York, 2007.

(43) Vacek, G.; Perry, J. K.; Langlois, J.-M. *Chem. Phys. Lett.* **1999**, *310*, 189–194.

Table 1. Crystallographic Data for **1** and **2**

	1	**2**
empirical formula	$C_{56}H_{76}N_{20}O_8Ni_4$	$C_{52}H_{68}N_{20}O_{12}Ni_4$
formula weight	1392.21	1400.10
crystal color	green	green
crystal system	monoclinic	monoclinic
space group	$P2_1$	$P2_1$
a [Å]	12.1087(8)	12.164(3)
b [Å]	20.8959(14)	21.065(5)
c [Å]	13.0900(9)	12.646(3)
α [°]	90.00	90.00
β [°]	111.190(2)	109.628(9)
γ [°]	90.00	90.00
V [Å^3]	3088.1(4)	3052.2(14)
Z	2	2
temperature [K]	293(2)	296(2)
2θ	3.34−57.96	3.42−54.06
μ [mm^{-1}]	1.271	1.291
ρ_{calcd} [g cm^{-3}]	1.497	1.523
$F(000)$	1456	1456
absorption-correction	multiscan	multiscan
index ranges	$-16 \leq h \leq 16$	$-15 \leq h \leq 15$
	$-28 \leq k \leq 27$	$-26 \leq k \leq 26$
	$-17 \leq l \leq 17$	$-16 \leq l \leq 16$
reflections collected	44 801	39 374
independent reflections (R_{int})	15 221(0.0417)	12 075(0.0501)
$R_1{}^a$/ w$R_2{}^b$ ($I > 2\sigma(I)$)	0.0400/0.1043	0.0441/0.1163
$R_1{}^a$/ w$R_2{}^b$ (for all data)	0.0537/0.1150	0.0659/0.1336

^{a} $R_1 = [\sum |F_o| - |F_c| / \sum |F_o|]$. ^{b} w$R_2 = [\sum w(F_o{}^2 - F_c{}^2)^2/\sum wF_o{}^4]^{1/2}$.

color of the solution changed from red to green. Afterward, Et$_3$N (0.101 g, 1 mmol) dissolved in 2 mL of MeOH was also added drop by drop, making the solution back to red. After 1 h, an aqueous solution (5 mL) of NaN$_3$ (0.260 g, 4 mmol) was added dropwise into the mixture, ending with a green color solution. Finally, after stirring for 2 h the solution was filtered and allowed to evaporate at room temperature. After a few days, green powdered compound was deposited, which was collected by filtration and washed with cold methanol. Recrystallization from methanol provided green, quality crystals. The deposited crystalline compound was collected by filtration and washed with cold methanol. Yield: 0.297 g (85%). Anal. calcd for C$_{56}$-H$_{84}$N$_{20}$O$_8$Ni$_4$: C, 48.04; H, 6.05; N, 20.01. Found: C, 48.31; H, 5.78; N, 20.02. Selected FT-IR data on KBr (cm^{-1}): ν(H$_2$O), 3410 m; ν(azide), 2073vs; ν(C=N), 1648 m.

Data of 2. Yield: 0.246 g (70%). Anal. calcd for C$_{52}$H$_{76}$N$_{20}$-O$_{12}$Ni$_4$: C, 44.36; H, 5.44; N, 19.89. Found: C, 44.31; H, 5.68; N, 19.81. Selected FT-IR data on KBr (cm^{-1}): ν(H$_2$O), 3399 m; ν(azide), 2069vs; ν(C=N), 1648 m.

Crystal Structure Determination of 1 and 2. The crystallographic data for **1** and **2** are summarized in Table 1. Diffraction data were collected on a Bruker-APEX II SMART CCD diffractometer at 293 K (for **1**) and at 296 K (for **2**), respectively, using graphite-monochromated Mo Kα radiation (λ = 0.71073 Å). For data processing and absorption correction the packages SAINT[44a] and SADABS[44b] were used. The structure was solved by direct and Fourier methods and refined by full-matrix least-squares based on F^2 using SHELXTL[44c] and SHELXL-97[44d] packages. Eight water hydrogen atoms for both **1** and **2** were not located. All other hydrogen atoms in **1** and **2** were inserted at calculated positions with isotropic thermal parameters and refined. Using anisotropic treatment for the nonhydrogen atoms and isotropic treatment for the hydrogen atoms, the final refinements converged at the R_1 values ($I > 2\sigma(I)$) 0.0400 and 0.0441 for **1** and **2**, respectively.

Results and Discussion

Description of the Structures of 1 and 2. Crystal structures of [{Ni^{II}(L^1)($\mu_{1,3}$-N$_3$)(H$_2$O)}$_4$] (**1**) and [{Ni^{II}(L^2)($\mu_{1,3}$-N$_3$)(H$_2$O)}$_4$] (**2**) are shown in Figures 1 and 2, respectively,
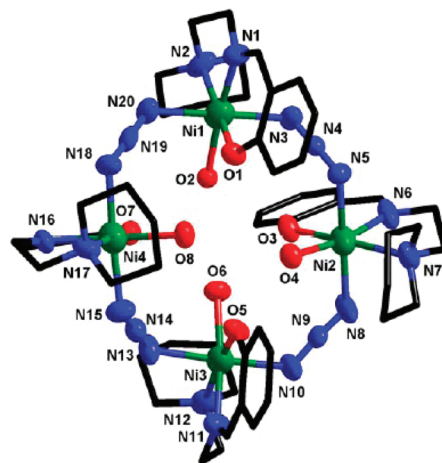
Figure 1. Crystal structure of [{Ni^{II}(L^1)$_{(1,3}$-N$_3$)(H$_2$O)}$_4$] (**1**). Ni (99%), N (85%), and O (85%) atoms are presented as ellipsoids, while C atoms are presented as wires/sticks. All the hydrogen atoms are omitted for clarity.
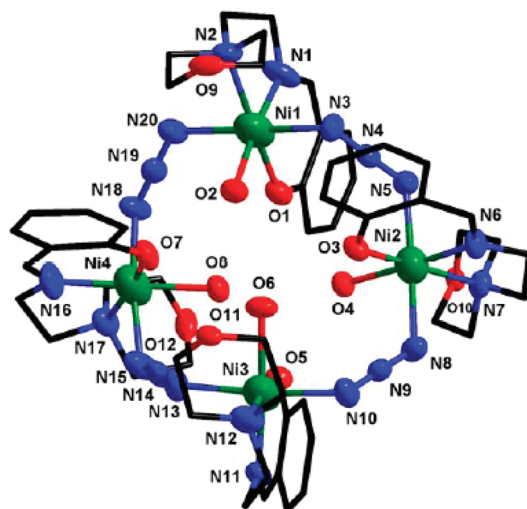
Figure 2. Crystal structure of [{Ni^{II}(L^2)$_{(1,3}$-N$_3$)(H$_2$O)}$_4$] (**2**). Ni (90%), N (50%), and O (50% for O1−O8, 15% for O9−O12) atoms are presented as ellipsoids, while C atoms are presented as wires/sticks. All the hydrogen atoms are omitted for clarity.

while the selected bond lengths and angles of both the compounds are listed in Table 2. The crystallographic data of both compounds reveal that these are tetranickel(II) compounds, in which each nickel(II) ion is surrounded by similar set of donor atoms. Each of the metal centers is coordinated to the phenoxo oxygen and the imine nitrogen and the piperidine or morpholine (for **1** and **2**, respectively) nitrogen atoms of one deprotonated ligand, [L^1]$^-$ or [L^2]$^-$, in the cases of **1** or **2**, respectively. The remaining coordination positions of the hexacoordinated nickel(II) centers are satisfied by one water oxygen atom and two nitrogen atoms of two EE bridging azide anions, that connect each nickel with two others. Eventually, each of the four azide anions bridges a pair of nickel(II) ions to result in the formation of a cyclic Ni$^{II}_4$ cluster in the title compounds. Overall, it is relevant to stress that the

(44) (a) *APEX-II*, *SAINT-Plus*, and *TWINABS*; Bruker−Nonius AXS, Inc.: Madison, WI, 2004 (b) Sheldrick, G. M. *SAINT-Plus*, version 6.02 and *SADABS*, version 2.03; Bruker AXS, lnc.: Madison, WI, 2002. (c) *SHELXTL*, version 6.10; Bruker AXS Inc.: Madison, WI, 2002. (d) Sheldrick, G. M. *SHELXL-97*; University of Göttingen: Göttingen, Germany, 1997.

Table 2. Selected Bond Lengths (Å) and Angles (°) of **1** and **2**

	1	**2**		**1**	**2**
Ni(1)			**Ni(2)**		
Ni(1)−O(1)	2.057(2)	2.068(4)	Ni(2)−O(3)	2.077(2)	2.050(4)
Ni(1)−N(2)	2.225(3)	2.306(5)	Ni(2)−N(7)	2.254(3)	2.260(4)
Ni(1)−N(1)	2.000(3)	1.973(5)	Ni(2)−N(6)	1.991(3)	1.992(4)
Ni(1)−N(3)	2.133(3)	2.105(5)	Ni(2)−N(8)	2.054(3)	2.120(5)
Ni(1)−N(20)	2.091(3)	2.088(5)	Ni(2)−N(5)	2.108(3)	2.147(5)
Ni(1)−O(2)	2.074(2)	2.060(3)	Ni(2)−O(4)	2.063(3)	2.071(3)
O(1)−Ni(1)−N(2)	173.48(11)	172.49(17)	O(3)−Ni(2)−N(7)	170.70(13)	173.31(17)
N(1)−Ni(1)−O(2)	175.11(11)	174.4(2)	N(6)−Ni(2)−O(4)	169.52(13)	177.36(17)
N(3)−Ni(1)−N(20)	175.66(13)	172.6(2)	N(5)−Ni(2)−N(8)	174.31(17)	174.8(2)
O(1)−Ni(1)−N(1)	91.32(12)	91.1(2)	O(3)−Ni(2)−N(6)	89.40(11)	91.86(18)
O(1)−Ni(1)−N(3)	91.23(11)	92.77(16)	O(3)−Ni(2)−N(8)	89.68(14)	91.47(17)
O(1)−Ni(1)−N(20)	92.11(11)	92.71(18)	O(3)−Ni(2)−N(5)	94.40(10)	90.80(16)
O(1)−Ni(1)−O(2)	86.06(9)	86.60(14)	O(3)−Ni(2)−O(4)	86.55(10)	86.43(14)
N(1)−Ni(1)−N(2)	83.06(13)	81.9(2)	N(6)−Ni(2)−N(7)	82.76(14)	81.82(18)
N(1)−Ni(1)−N(3)	87.49(13)	89.1(2)	N(6)−Ni(2)−N(8)	97.10(15)	94.8(2)
N(1)−Ni(1)−N(20)	95.21(13)	95.8(2)	N(6)−Ni(2)−N(5)	86.92(13)	89.78(19)
N(2)−Ni(1)−N(3)	91.82(12)	89.91(18)	N(7)−Ni(2)−N(8)	86.34(16)	86.93(18)
N(2)−Ni(1)−N(20)	85.14(12)	85.27(19)	N(7)−Ni(2)−N(5)	90.19(13)	91.34(17)
N(2)−Ni(1)−O(2)	99.78(11)	100.60(17)	N(7)−Ni(2)−O(4)	102.01(12)	99.97(16)
N(3)−Ni(1)−O(2)	88.43(11)	85.95(18)	N(8)−Ni(2)−O(4)	92.55(13)	87.23(18)
N(20)−Ni(1)−O(2)	89.03(11)	89.36(17)	N(5)−Ni(2)−O(4)	83.76(11)	88.24(16)
Ni(3)			**Ni(4)**		
Ni(3)−O(5)	2.064(2)	2.059(4)	Ni(4)−O(7)	2.072(2)	2.051(4)
Ni(3)−N(12)	2.290(3)	2.293(5)	Ni(4)−N(17)	2.249(3)	2.294(5)
Ni(3)−N(11)	1.989(3)	2.002(4)	Ni(4)−N(16)	1.999(3)	1.981(5)
Ni(3)−N(13)	2.071(3)	2.114(5)	Ni(4)−N(18)	2.088(3)	2.101(4)
Ni(3)−N(10)	2.079(3)	2.095(5)	Ni(4)−N(15)	2.108(3)	2.090(5)
Ni(3)−O(6)	2.089(2)	2.098(3)	Ni(4)−O(8)	2.083(2)	2.067(4)
O(5)−Ni(3)−N(12)	173.17(11)	173.55(17)	O(7)−Ni(4)−N(17)	173.28(10)	172.64(17)
N(11)−Ni(3)−O(6)	173.87(13)	176.14(18)	N(16)−Ni(4)−O(8)	177.21(12)	178.0(2)
N(10)−Ni(3)−N(13)	175.82(18)	173.3(2)	N(15)−Ni(4)−N(18)	174.57(13)	171.5(3)
O(5)−Ni(3)−N(11)	90.86(12)	91.15(18)	O(7)−Ni(4)−N(16)	91.07(11)	91.0(2)
O(5)−Ni(3)−N(13)	90.20(11)	90.63(18)	O(7)−Ni(4)−N(18)	92.65(11)	93.29(18)
O(5)−Ni(3)−N(10)	91.62(15)	91.91(19)	O(7)−Ni(4)−N(15)	90.76(11)	90.3(2)
O(5)−Ni(3)−O(6)	86.00(9)	86.78(14)	O(7)−Ni(4)−O(8)	86.30(9)	87.02(15)
N(11)−Ni(3)−N(12)	82.74(13)	82.9(2)	N(16)−Ni(4)−N(17)	83.29(13)	81.9(2)
N(11)−Ni(3)−N(13)	90.92(14)	91.3(2)	N(16)−Ni(4)−N(18)	91.47(13)	92.5(2)
N(11)−Ni(3)−N(10)	92.81(16)	94.81(19)	N(16)−Ni(4)−N(15)	92.68(13)	95.1(2)
N(12)−Ni(3)−N(13)	92.25(12)	91.9(2)	N(17)−Ni(4)−N(18)	91.14(12)	89.08(18)
N(12)−Ni(3)−N(10)	86.37(15)	86.2(2)	N(17)−Ni(4)−N(15)	85.88(12)	88.3(2)
N(12)−Ni(3)−O(6)	100.59(11)	99.33(17)	N(17)−Ni(4)−O(8)	99.28(11)	100.04(17)
N(13)−Ni(3)−O(6)	83.84(12)	85.48(19)	N(18)−Ni(4)−O(8)	89.57(11)	87.64(18)
N(10)−Ni(3)−O(6)	92.53(14)	88.51(18)	N(15)−Ni(4)−O(8)	86.44(12)	84.9(2)

intralinking of the four metal ions in the cluster takes place only by the four EE azide anions.

The distance ranges of the metal−ligand bonds are rather wide. However, on average the distances of the four metal centers are not very different, 2.000(3)−2.225(3) Å for Ni(1), 1.991(3)−2.254(3) Å for Ni(2), 1.989(3)−2.290(3) Å for Ni(3), and 1.999(3)−2.249(3) Å for Ni(4) in **1** and 1.973(5)−2.306(5) Å for Ni(1), 1.992(4)−2.260(4) Å for Ni(2), 2.002(4)−2.293(5) Å for Ni(3), and 1.981(5)−2.294(5) Å for Ni(4) in **2**. For each Ni^{II} center, the bond length involving the imine nitrogen is always the shortest (1.989(3)−2.000(3) Å in **1** and 1.973(5)−2.002(4) Å in **2**), while the Ni−N(piperidine/morpholine) is the longest (2.225(3)−2.290(3) Å in **1** and 2.260(4)−2.306(5) Å in **2**). The metal−water, metal−phenoxo, and metal−azide bond distances are intermediate and lie in the ranges of 2.063(3)−2.089(2), 2.057(2)−2.077(2), and 2.054(3)−2.133-(3) Å, respectively, in **1** and 2.060(3)−2.098(3), 2.050(4)−2.068(4), and 2.088(5)−2.147(5) Å, in that order, for **2**.

It is evident, from the mentioned large bond lengths, that the hexacoordinated environment of all the four metal centers in both the compounds is distorted octahedral. The distortion can be further evidenced from the deviation of both the cisoid and transoid angles from the ideal values. The N(azide)−Ni−N(azide) angles for all the metal centers in compounds **1** and **2** lie in the range of 171.5(3)−175.8(2)°, indicating trans arrangement of the two EE azido ligands within the coordination environment of all the Ni^{II} centers. It is worth mentioning that such trans arrangement has been previously observed in a number of 1D nickel(II) systems,[4,21,24,25] although here appears as the only coordinator motive in a cluster (0D) feature crystallographically unprecedented until now.

Numerous azido-bridged metal clusters having nuclearity three or higher have been already reported in the literature. These systems can be classified in two broad classes: only azido-[4,15,16] or heterobridged clusters[4,11−14,19,23,27−29] (where the metal ions are additionally bridged by other bridging moieties). Among those, the number of compounds that form the first type (exclusively azido ligands) is very limited compared with the second group. In addition, while several bridging modes of azido ligand

Table 3. Ni−N−N Angles (°) and Ni−N···N−Ni Torsion Angle (°) in **1** and **2**

	1	**2**
Ni(1)−N(3)−N(4)	117.0(2)	120.2(4)
Ni(1)−N(20)−N(19)	123.1(2)	122.0(4)
Ni(2)−N(5)−N(4)	116.1(2)	118.0(4)
Ni(2)−N(8)−N(9)	129.7(3)	123.3(4)
Ni(3)−N(10)−N(9)	123.8(3)	122.6(4)
Ni(3)−N(13)−N(14)	121.6(2)	122.3(4)
Ni(4)−N(15)−N(14)	121.4(3)	121.2(5)
Ni(4)−N(18)−N(19)	123.3(2)	120.9(4)
Ni(1)−N_3−Ni(2)	90.6	85.4
Ni(2)−N_3−Ni(3)	3.3	54.7
Ni(3)−N_3−Ni(4)	87.5	86.1
Ni(4)−N_3−Ni(1)	50.4	57.8

($\mu_{1,1}$-;[4,11] $\mu_{1,3}$-;[23] $\mu_{1,1,1}$-;[27] $\mu_{1,1,3}$-;[29] $\mu_{1,1}$- and $\mu_{1,3}$-;[12] $\mu_{1,1}$- and $\mu_{1,1,1}$-;[13] $\mu_{1,1}$- and $\mu_{1,1,3}$-;[14] $\mu_{1,3}$- and $\mu_{1,1,3}$-;[19] $\mu_{1,1,1}$- and $\mu_{1,1,3}$-[28]) have been observed in heterobridged clusters, only few bridging modes ($\mu_{1,1}$-;[4,15] $\mu_{1,1}$-, and $\mu_{1,1,1}$-[16]) have been described in the case of the first group. Previous to this paper only a trinuclear cluster described by extended X-ray absorption fine structure (EXAFS) has exhibited a $\mu_{1,3}$-azido coordination mode as the exclusive coordination ligand.[21b] Clearly, the tetranickel(II) cluster compounds crystallographically described here, [{Ni[II]-(L[1])($\mu_{1,3}$-N_3)(H_2O)}$_4$] (**1**) and [{Ni[II](L[2])($\mu_{1,3}$-N_3)(H_2O)}$_4$] (**2**), resulting from only a $\mu_{1,3}$-azide bridging ligand represent a unique family of tetranuclear azido-bridged clusters.

On the other hand, while comparing compounds **1** and **2** not only several similarities can be found but also relevant differences. This way, both Ni[II]$_4$ clusters are cyclic, with N−N distances and N−N−N angles in the azide anions of 1.148(4)−1.189(4) Å and 175.8(4)−179.2(3)° for **1** and 1.163(7)−1.182(6) Å and 177.2(7)−178.2(6)° for complex **2**, indicating that the azide is roughly linear and has roughly the same N−N bond lengths. The Ni−N−N angles are considerably bent in both compounds, with values between 116.1(2)−129.7(3)° in **1** and 118.0(4)−123.3(4)° in **2** (Table 3). The four intramolecular Ni···Ni distances are slightly different: the Ni(1)···Ni(2), Ni(2)···Ni(3), Ni(3)···Ni(4), and Ni(4)···Ni(1) distances are, respectively, 5.049, 5.195, 4.884, and 4.931 Å in **1** and 5.115, 4.949, 5.190, and 4.883 Å in **2**. The Ni···Ni···Ni angles in the cluster lie in the range 85.7−90.4° in **1** and 85.1−88.8° in **2**. The arrangement of the four nickel(II) centers in each title compound can be considered as a quasi-square. As listed in Table 3, the four Ni−N···N−Ni torsion angles (τ; 3.3, 50.4, 87.5, and 90.6°) between the two least-squares NiN_3 planes, in a particular nickel(II)−azide−nickel(II) fragment, vary in the wide range of 3.3−90.6° in **1**. In contrast, the four τ values in compound **2** are 54.7, 57.8, 85.4, and 86.1°. Clearly, despite having a similar type of structure, the two azide-bridged tetranickel(II) compounds are significantly different in terms of the Ni−N···N−Ni torsion angles, which is the key parameter to govern the magnetic behavior (vide infra).

Syntheses and FT-IR Spectra. The two title compounds **1** and **2** were readily prepared in high yield on reacting nickel(II) perchlorate hexahydrate, triethyl amine, and sodium azide with the solution containing salicylaldehyde and 1-(2-aminoethyl)-piperidine or 4-(2-aminoethyl)-morpholine (for **1** or **2**, respectively). As already discussed, both the compounds are tetranuclear clusters containing
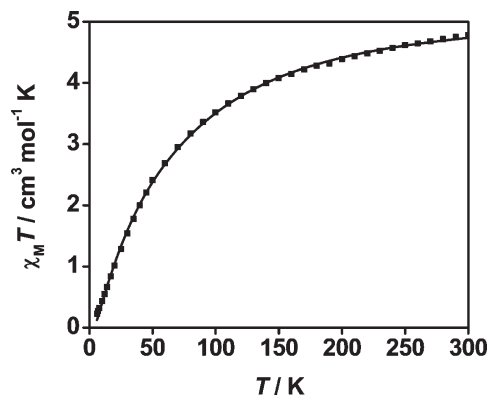
Figure 3. Observed $\chi_M T$ vs T plots for complex **1** is shown as solid square symbols. The solid line represents the best fitting to the experimental data between 10 and 300 K.

1:1 stoichiometric ratio of Ni[II] and [L[1]][−]/[L[2]][−]. All the three donor centers, phenolate oxygen atom and imine and piperidine/morpholine nitrogen atoms, of a ligand are monodentate and coordinate to one metal center. It may be mentioned that there are a number of nickel(II)−azide compounds derived from closely similar ligands. In a few of these, the phenoxo oxygen atom of the Schiff base ligand acts as a bridging center to generate either dinuclear or trinuclear compounds.[45] On the other hand, the Schiff base in most of the nickel(II)−azide compounds behaves as a tridentate blocking ligand to produce a 1D system[46] in one case and a mononuclear species in all other cases.[47] Clearly, the behavior of [L[1]][−]/[L[2]][−] as a blocking ligand in the present investigation is very much common. Albeit, as discussed, the final topology in **1** and **2** is unprecedented, which indicates the success of the synthetic strategy to achieve novel metallo-azide topology.

The characteristic azide stretching in **1** and **2** is very strong and appears at 2073 and 2069 cm^{−1}, respectively. The imine stretching in **1** and **2** is observed as a medium intensity band at 1648 cm^{−1}. The presence of water molecules is evident from the appearance of a medium intensity band at 3410 and 3399 cm^{−1} for **1** and **2**, respectively.

Magnetic Properties. DC magnetic susceptibility data were collected for crushed crystalline samples of **1** and **2** with applied magnetic fields of 0.04 and 0.7 T (from 2 to 30 and 30 to 300 K, respectively). The data are shown in Figures 3 and 4, in the same order, as $\chi_M T$ versus T plots.

For compound **1**, the $\chi_M T$ value, 4.72 cm[3] mol^{−1} K, at 300 K is above the expected value of 4.0 cm[3] mol^{−1} K for four independent Ni[II] ions with $g = 2.0$ and $S = 1$. As temperature decreases, the $\chi_M T$ product decreases gradually to nearly zero, 0.08 cm[3] mol^{−1} K, at 2 K. These features are indicative of an overall antiferromagnetic behavior, alike most Ni[II] complexes containing azido linkers with EE bridging modes.[4,7,19,21b,c,22]

(45) (a) Qiu, X.-Y.; Liu, W.-S.; Zhu, H.-L. *Z. Anorg. Allg. Chem.* **2007**, *633*, 1480–1484. (b) Cao, G.-B. *Synth. React. Inorg., Met.-Org., Nano-Met. Chem.* **2007**, *37*, 639–642.

(46) Sun, Y.-X. *Acta Crystallogr., Sect. E: Struct. Rep. Online* **2006**, *62*, m109–m111.

(47) (a) Li, K.; Huang, S.-S.; Zhang, B.-J.; Meng, D.-L.; Diao, Y.-P. *Acta Crystallogr., Sect. E: Struct. Rep. Online* **2007**, *63*, m2291. (b) Diao, Y.-P.; Huang, S.-S.; Zhang, B.-J.; Li, K. *Acta Crystallogr., Sect. E: Struct. Rep. Online* **2007**, *63*, m2495. (c) Zhou, Z.; Xiao, Z.-H. *Acta Crystallogr., Sect. E: Struct. Rep. Online* **2007**, *63*, m2012.
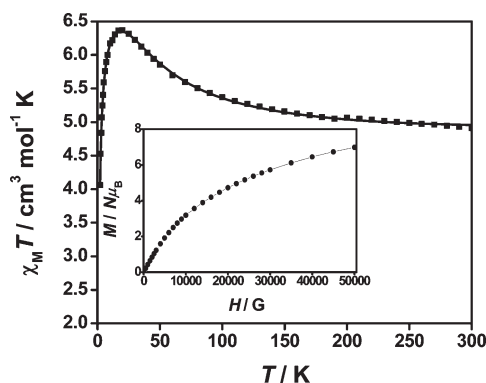
Figure 4. Observed $\chi_M T$ vs T plot of complex **2** is shown as solid square symbols. The solid line represents the best fit from 2 to 300 K. The inset is an isothermal $M/N\mu_B$ vs H/G plot at 2.0 K.

In the past, changes of the torsion angle in a dinuclear Ni^{II} complex containing one 1,3-μ-azido and one pyrazolate group as bridging ligands have been proved the cause of magnetic bistability of such system.[23b] Due to the novelty of compound **1**, strict comparison and discussion of the magnetic response with analogous clusters is not available. However, a number of data is already described for related 1D trans-Ni^{II}−(μ-N_3)−Ni systems.[4,21,24,25] According to the magneto-structural correlations made on these systems, Ni−N−N and torsion (τ, described as Ni−N···N−Ni) angles are the main factors to determine the nature and strength of the exchange interactions. In the present work, the Ni−N−N angles (116.1−129.7°) for all four Ni^{II} centers in **1** are not very different and comparable to others found in the literature.[4,21,24,25] In general, for Ni−N−N angles close to 108° strong antiferromagnetic interaction will be expected, meanwhile angles nearby 164° will exhibit accidental orthogonality resulting in ferromagnetic interactions. Compound **1** shows intermediate values of those which may emphasize the weakness of the total magnetic interaction. However, more drastic variations were found in the four τ angles, with values: 3.3, 50.4, 87.5, and 90.6°. This information was used as criterion to define the final magnetic system. Fitting of the data was performed using the MAGPACK package[48] and carried out by means of the marked differences among the torsion angles; for that, three exchange coupling constants were considered in the following Heisenberg-spin Hamiltonian, $\hat{H} = -J_a(\hat{S}_1\hat{S}_2 + \hat{S}_3\hat{S}_4) - J_b\hat{S}_2\hat{S}_3 - J_c\hat{S}_4\hat{S}_1$ (numbering of the spins were made according to crystallographic criteria). Only experimental points from 10 to 300 K were considered in the magnetic analysis due to a small impurity (commonly observed at the lowest temperatures in antiferromagnetic Ni-azido systems). Thus, diagonalization of the full matrix was performed, and the magnetic answer of the four-member Ni^{II} ring analyzed. Least-squares fitting of the experimental data led to the following parameters: $J_a = 35.5$, $J_b = -70.5$, and $J_c = -15.5$ cm^{-1} and $g = 2.29$, with $R = 8.5 \times 10^{-5}$.

These results are indicative of a moderate antiferromagnetic behavior of compound **1** in agreement with the

(48) (a) Borrás-Almenar, J. J.; Clemente-Juan, J. M.; Coronado, E.; Tsukerblat, B. S. *Inorg. Chem.* **1999**, *38*, 6081–6088. (b) Borrás-Almenar, J. J.; Clemente-Juan, J. M.; Coronado, E.; Tsukerblat, B. S. *J. Comput. Chem.* **2001**, *22*, 985–991.

Table 4. Structural Parameters (in Å and °) and Calculated Exchange Coupling Constants Corresponding the Two Ni^{II}_4 Complexes **1** and **2**

|	d(Ni···Ni)	d(Ni−N)$_{av}$	Ni−N−N	Ni−N···N−Ni	J_{calcd}
1					
J_{12}	5.049	2.120	117.0(2), 116.1(2)	90.6	+14.9
J_{23}	5.195	2.066	129.7(3), 123.8(3)	3.3	−85.3
J_{34}	4.884	2.090	121.6(2), 121.4(3)	87.5	+17.1
J_{41}	4.931	2.090	123.3(2), 123.1(2)	50.4	−18.6
2					
J_{12}	5.115	2.126	120.2(4), 118.0(4)	85.4	+14.1
J_{23}	4.949	2.108	123.3(4), 122.6(4)	54.7	−4.5
J_{34}	5.190	2.101	122.3(4), 121.2(5)	86.1	+15.5
J_{41}	4.883	2.095	122.0(4), 120.9(4)	57.8	−1.2

shape of the curve. In general, when τ increases from 0°, the pathway becomes less effective, decreasing the strength of the exchange interaction (less antiferromagnetic). Following this idea, complex **1** exhibits two high values of τ (87.5 and 90.6°), which are related to the ferromagnetic exchange (J_a), one intermediate of ≈50° antiferromagnetic but not very strong (J_c), and finally one lower τ of 3.3° (unprecedented in polynuclear clusters until now) that is associated to the strongest intramolecular antiferromagnetic interaction (J_b). Herein, the antiferromagentic exchanges prevail, and the final spin ground state of the system is $S = 0$.

On the other hand, the room-temperature value of $\chi_M T$ for compound **2** is 4.90 cm^3 mol^{-1} K (higher than the value expected for four uncorrelated $S = 1$ spins). This value increases up to a maximum of 6.37 cm^3 mol^{-1} K at 20 K, after which it decreases abruptly at lower temperatures, down to 4.06 cm^3 mol^{-1} K at 2.0 K. These results suggest the presence of ferromagnetic intramolecular interactions, although the value of the total spin ground state was not evident and needed further analysis of the data. Using the program mentioned above and taking into account the parameters discussed before (for compound **2**: Ni−N−N values are between 118.0 and 123.3° and τ are 54.7, 57.8, 85.4, and 86.1°), the system was better described using two J values. The calculation of the exchange coupling interactions is based on the following Hamiltonian: $\hat{H} = -J_a(\hat{S}_1\hat{S}_2 + \hat{S}_3\hat{S}_4) - J_b\hat{S}_2\hat{S}_3 - J_c\hat{S}_4\hat{S}_1$. The fitting results are shown in Figure 4 in the form of solid lines, and the values obtained were: $J_a = +21.6$ and $J_b = -1.17$ cm^{-1}, $g = 2.12$, and TIP = 522×10^{-6} cm^3 mol^{-1}, with $R = 1.0 \times 10^{-5}$. In this regard, J_a and J_b are related to the τ values 85.4°/86.1° and 54.7°/57.8°, respectively. To get more insight on the spin ground state of the complex, magnetization studies were performed (inset of Figure 4), although the curve did not reach saturation, and therefore the nature of this could not be established. Final conclusions on that matter were obtained from DFT calculations (see below).

Electronic Structure Calculations. The use of theoretical methods allows to calculate and also to understand the dependence of the exchange coupling constants with structural changes. In the past, some of us have previously studied such dependences for some azido-bridging ligands: Cu^{II} and Ni^{II} complexes with a double EO[32a,b] or EE bridging ligands.[32c,d] For compounds **1** and **2**, the existence of four J values makes it considerably difficult to get an
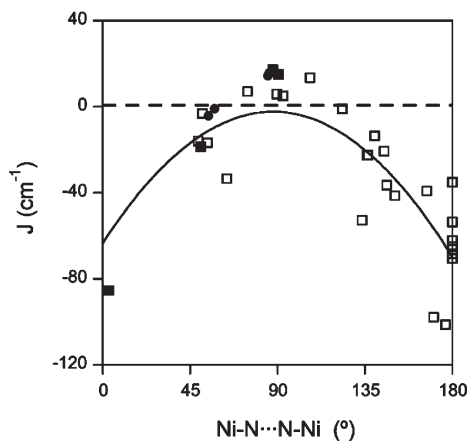
Figure 5. Dependence of the exchange coupling constants for the complexes with a Ni−N−N angle below 135° (white squares, Table 5) and those obtained with the DFT calculations for the complexes **1** and **2** (black squares and circles, respectively).

accurate fitting of the magnetic susceptibility curve. Thus, in order to estimate each interaction we have to perform electronic structure calculations using methods based on DFT (see Computational Details). This approach allows the resolution of all the exchange interactions present in the molecule, and for that, the Hamiltonian employed was the following:

$$\hat{H} = -J_{12}\hat{S}_1\hat{S}_2 - J_{23}\hat{S}_2\hat{S}_3 - J_{34}\hat{S}_3\hat{S}_4 - J_{41}\hat{S}_4\hat{S}_1 \quad (1)$$

The calculated J values together with the most relevant structural parameters for the exchange interactions of these two complexes are collected in Table 4. As it can be observed from these values, there is a nice agreement with the experimentally fitted J values, thus, the predominance of the antiferromagnetism in complex **1**, especially due to the J_{23} interaction. While for complex **2**, the system is close to be completely ferromagnetic, but two interactions are still slightly antiferromagnetic.

Table 5. Cambridge Structural Database Refcodes,[49] Structural Parameters (in Å and °), and Experimental Exchange Coupling constants (in cm^{-1}) for the Nickel Complexes Containing a Single EE Azido-Bridging Ligand

refcode	d(Ni⋯Ni)	d(Ni−N)$_{av}$	Ni−N−N	Ni−N⋯N−Ni	J_{exp}	ref
		Molecular Systems with Only EE Azido-Bridging Ligands				
LIJCUC	6.073	2.132	131.6, 131.6	180.0	−53.6	22a
WOHMUB	6.188	2.122	139.4, 139.4	180.0	−40.9	22b
		Molecular Systems with Also Other Bridging Ligands				
ICULAT	5.322	2.149	126.7, 123.8	74.6	+7.1	23a
KENBIP	5.472	2.018	126.3, 133.5	89.6	+6.0	12
KERYIQ	5.480	2.028	126.0, 134.7	92.9	+5.0	12
YABNEV	5.788	2.031	148.1, 141.7	36.1	−32.4	18e
		Chain Structures with only EE Azido-Bridging Ligands				
ACAGEQ	5.662	2.110	124.5, 133.3	106.8	+13.5	24a
AGOXAV	6.112	2.123	135.6, 135.6	180.0	−35.0	24b
	5.950	2.100	128.6, 128.6	180.0	−65.0	
	5.950	2.112	140.3, 128,6	133.5	−52.7	
CIBBOF	5.820	2.189	116.0, 117.0	171.0	−63.7	26a
	5.340	2.106	131.9, 126.5	64.0	−33.4	
CIBBUL	6.141	2.088	138.8, 138.8	179.9	−26.8	26a
	6.111	2.101	135.8, 135.8	180.0		
GUNQEL	5.618	1.884	134.8, 134.8	180.0	−68.4	21c
	5.603	1.863	143.7, 143.7	180.0	−37.8	
GUNQIP	5.908	2.150	123.4, 134.8	140.0	−13.6	21c
HECQAH	5.717	2.111	128.4, 146.1	75.8	+6.91	21d
HEWNEC	5.648	2.108	123.7, 120.1	133.8	−33.0	26b
	6.111	2.109	121.3, 126.6	138.9		
HEWNIG	5.665	2.101	122.6, 122.6	134.9	−22.4	26b
	5.741	2.112	127.4, 120.7	138.0		
JUXYAC	6.149	2.168	128.3, 140.3	166.9	−39.2	24c
LUWXIK	6.146	2.167	135.6, 135.6	144.9	−20.7	24d
PEZMIR	5.602	2.123	126.6, 144.6	49.2	−16.0	24e
PITMAG	6.003	2.204	123.6, 123.6	180.0	−62.1	25a
	6.128	2.078	142.4, 142.4	180.0		
PITMEK	6.182	2.133	151.8, 151.3	180.0	−18.5	25a
RELLEZ	6.139	2.125	136.6, 136.6	180.0	−41.1	25b
RELLID	5.983	2.122	126.1, 126.1	180.0	−70.6	25b
WIBDAM	6.067	2.179	130.6, 128.5	150.5	−41.4	25c
	6.067	2.169	131.5, 131.5	146.2	−36.4	
WIBDIU	5.797	2.144	122.9, 122.9	175.5	−101.4	25c
	5.769	2.158	116.5, 116.5	177.6		
WUJTEA	6.155	2.117	136.2, 149.8	161.1	−21.8	25d
WUJTIE	6.385	2.122	151.4, 151.4	179.9	−3.2	25d
WUJTOK	6.190	2.112	145.4, 136.5	177.6	−42.3	25d
YOGJUZ01	5.770	2.165	117.2, 117.2	170.4	−97.8	25e
ZOLLIV	5.313	2.152	125.9, 131.8	53.9	−16.8	25f
ZOLLOB	5.335	2.172	122.6, 135.0	51.4	−3.25	25f
ZOVLEB	5.864	2.183	126.2, 127.9	123.4	−1.0	26c

Scheme 2. Relative Orientation of the Magnetic Orbitals of Ni^{II} and π Orbitals of Azido Ligand
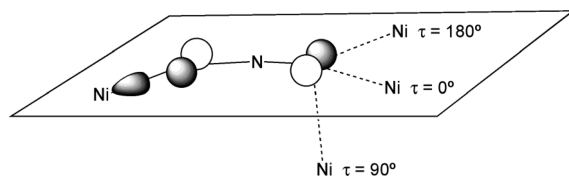
As mentioned before, two structural factors that control the magnetic behavior in single μ-1,3 azido-bridging ligands are the Ni−N−N and torsion (τ) angles.[4,21,24,25] For the two studied complexes, **1** and **2**, the Ni−N−N angle values are rather similar, thus, the changes in the magnetic response are mainly controlled by τ. Based on our studies, there is a nice correlation between the calculated J values and the Ni−N···N−Ni torsion angle. Thus, for τ values around 90°, the exchange interactions are ferromagnetic, while the exchange couplings become antiferromagnetic for torsion angle values smaller than 60° (or larger than 120°). This magneto-structural correlation (see Figure 5) can be clearly corroborated by comparing experimental J values collected from the literature for complexes with similar Ni−N−N angle values with those J parameters obtained in this work (Ni−N−N angle value below 135°, see Table 5). It is worth noting that J_{23} (J_b in the fitting) interaction of complex **1** corresponds to a unique case where τ is almost 0° and consequently strongly antiferromagnetic. Finally, for this family of complexes, the analysis of J values versus Ni−N−N angles shows a decrease of the antiferromagnetic contribution when the angles increase. Thus, there is a linear correlation with Ni−N−N angles if one may compare J values that have similar τ ($\tau > 165°$, Figure S1, Supporting Information).

The mentioned magneto-structural correlation can be understood by considering the magnetic orbitals involved in the exchange interactions. The lobe of the d orbitals d_{z^2} or $d_{x^2-y^2}$ of the Ni^{II} cation, oriented toward the π orbital of the azido ligand in the Ni−N−N−N plane (see Scheme 2), can provide a maximum overlap (strongest antiferromagnetism) when a second Ni^{II} cation is placed with a Ni−N···N−Ni torsion angle of either 0° or 180°. However, if the torsion angle is 90°, then the two magnetic orbitals of the second Ni^{II} cation are orthogonal to the π orbital of the azido ligand, and consequently the coupling is ferromagnetic. The influence of the Ni−N−N can be easily explained because the increase of such an angle results in a smaller overlap between the d orbital of the Ni^{II} cation and the π orbital of the azido ligand, being strictly orthogonal for Ni−N−N equal to 180°.

Finally to corroborate these results, experimental magnetic susceptibility curves (white symbols, subtracting TIP for complex **2**; Figure 6) are plotted together with the magnetic data of complexes **1** and **2** using DFT J values (black symbols, using g = 2.29 and 2.0023 for **1** and **2**, respectively; Figure 6). The experimental and theoretical curves are in agreement, confirming the ability of the employed DFT methodology to reproduce the exchange interactions in this type of polynuclear complexes. The differences between the curves are due to the

(49) Allen, F. H. *Acta Crystallogr.* **2002**, *B58*, 380–388.
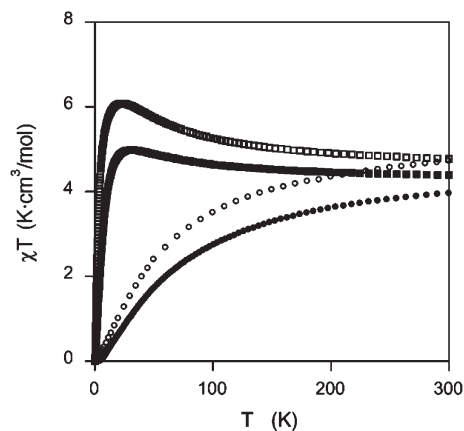
Figure 6. Dependence of the χT product with the temperature for the complexes **1** and **2**, squares and circles, respectively. The black symbols represent the values obtained from the DFT calculated J value (g = 2.29 and 2.0023 for **1** and **2**, respectively), while the white color corresponds to the measured susceptibility data eliminating the TIP for **2**.

very large sensitivity of the shape of the curve with the J values. Thus, such differences are due to small variations between calculated and measured J values. The presence of such small energy differences implies that even at very low temperatures these excited states are populated giving nonzero $\chi_M T$ values (see Figure 4). For instance, compound **2** exhibits a S = 0 ground state and a S = 1 excited state at less than 1 cm^{-1} above; furthermore, a S = 4 high spin state at only 6 cm^{-1} from the ground state.

Conclusions

Despite the extensive research on metal-azide chemistry that has been developed during the last 30 years, there are topologies that have not yet been achieved, among them, clusters having nuclearity of four or more and containing only EE azido groups as bridges were one of them. This is to a certain extent surprising and could be considered as a gap fulfilled in the present work by the achievement of compounds **1** and **2**. These two species are the sole examples of the only $\mu_{1,3}$-N$_3$-bridged Ni^{II} clusters, the title compounds [{Ni^{II}(L^1)($\mu_{1,3}$-N$_3$)(H$_2$O)}$_4$] (**1**) and [{Ni^{II}(L^2)($\mu_{1,3}$-N$_3$)-(H$_2$O)}$_4$] (**2**) represent a unique family of metal-azide compounds.

The two title compounds have been derived from two similar tridentate Schiff base ligands that also coordinate in an analogous way. The bridging network and the topology of the two complexes are alike too. In general, compounds **1** and **2**, showing both bond lengths and angles in the coordination environment of the metal ions, are comparable as well as the Ni−N−N angles. In spite of all these similarities, the two complexes differ significantly in terms of the Ni−N···N−Ni torsion angles (τ); 3.3, 50.4, 87.5, and 90.6° in **1** and 54.7, 57.8, 85.4, and 86.1° in **2**. One τ value of 3.3° in **1** is interesting because a τ value close to 0° is unprecedented in metal-azide chemistry.

The analyses of the measured magnetic susceptibility together with the results of the theoretical calculations using density functional theory methods show nice agreements for both complexes. Regardless of their similarities, complex **1** exhibits an overall antiferromagnetic behavior in contrast to complex **2** that shows ferromagnetic conduct. Previously, it was pointed out the importance of the Ni−N−N angle as a

key structural parameter in controlling the magnetic behavior of this type of complexes. However, for the two studied complexes, such angle values remain almost constant being the τ values crucial to control the magnetic properties. Both the ferromagnetic and antiferromagnetic pathways exist in the two complexes due to the wide range of τ values. This way, the antiferromagnetic behavior observed for complex **1** is mainly due to a low torsion angle (3.3°), while complex **2** is predominantly ferromagnetic because torsion angles are higher in value (between 50 and 90°). The overlap between the magnetic orbitals is relatively large when the τ value is close to 0°, while the strongest ferromagnetic coupling corresponding to an angle of 90° is due to the orthogonality of the orbitals. The intermediate situations, such as the τ values close to 50°, result in weak antiferromagnetic couplings.

Supporting Information Available: Crystallographic data of **1** and **2** in CIF format and Figure S1. These materials are available free of charge via the Internet at http://pubs.acs.org.

Note Added after ASAP Publication. This paper was published on the Web September 21, 2010, with minor text errors in the author affiliations. The corrected version was reposted on September 24, 2010.